nature communications

Article

https://doi.org/10.1038/s41467-024-55081-5

Association of structured continuum emission with dynamic aurora

Received: 17 April 2024

Accepted: 27 November 2024

Published online: 30 December 2024

Check for updates

E. Spanswick[1] ✉, J. Liang[1], J. Houghton[1], D. Chaddock[1], E. Donovan[1], B. Gallardo-Lacourt[2,3], C. Keenan[1], J. Rosehart[1], Y. Nishimura[4], D. Hampton[5] & M. Gillies[1,6]

Patterns of ionospheric luminosity provide a unique window into our complex, coupled space environment. The aurora, for example, indicates plasma processes occurring thousands of km away, depositing immense amounts of energy into our polar ionospheres. Here we show observations of structured continuum emission associated with the dynamic aurora. The presence of weak ambient continuum emission has long been recognized. However, studies of its relationship to aurora are scarce and limited by observational constraints. We use spectrally resolved measurements to analyze these previously unexplained emissions, adding critical information about spatial structure, characteristic spectra, and location within auroral dynamics. Our findings demonstrate that the coupling among auroral processes, the plasma, and the neutral atmosphere can unfold at meso-scales and is more complex than previously reported. We suggest that the meso-scale auroral precipitation may, under certain circumstances, effectively couple to atmospheric chemistry and conditions to produce the continuum structure.

To enter an excited state and emit photons, the atmospheric particle must gain energy. In classical aurora, the energy comes from the impact of energetic particle precipitation from the magnetosphere. Solar irradiation may serve as another main energy source and produce airglow[1]. Furthermore, certain chemical reactions in the atmosphere can release energy in the form of photons, producing the so-called chemiluminescence[2].

The presence of a continuum emission component in the night sky has long been recognized[3,4]. In particular, Sternberg and Ingham[4] presented a quantitative investigation of weak ambient continuum emissions in the night sky. Such continuum emission was understood to be the result of chemiluminescence. Reports on continuum emission associated with aurora are scarce and limited to event studies[5,6]. For example, Gattinger and Jones[6] noticed the strong, unexplained presence of a continuum emission component in their observed auroral spectra. In recent years, the discovery and observations of the Strong Thermal Emission Velocity Enhancement (STEVE)[7] have rejuvenated interest in continuum emission. A major component of STEVE emissions is not from known atomic or molecular auroral optical emissions but is instead made of a continuum emission[8,9]. The underlying mechanisms responsible for the STEVE emission are not entirely clear but are commonly speculated as chemiluminescence enabled by extreme heating in the ionosphere in association with intense sub-auroral ion drifts[10,11].

Recently deployed Transition Region Explorer (TREx) high-resolution, broad-band color auroral imager network (TREx-RGB[12]) provides a systematic auroral imaging dataset that affords a measure of continuum emission observations. Historical scientific imaging of structured aurora and airglow traditionally employs cameras utilizing narrow-band optical filters. The advantage of this approach is that it produces continuous datasets of calibrated luminosity within a

[1]Department of Physics and Astronomy, University of Calgary, 2500 University Drive N.W., Calgary T2N 1N4 AB, Canada. [2]NASA Goddard Space Flight Center, 8800 Greenbelt Rd, Greenbelt 20771 MD, USA. [3]Department of Physics, The Catholic University of America, 620 Michigan Ave., N.E., Washington 20064 DC, USA. [4]Department of Electrical and Computer Engineering, Boston University, 725 Commonwealth Avenue, Boston 02215 MA, USA. [5]Geophysical Institute, University of Alaska Fairbanks, 1731 South Chandalar Dr., Fairbanks 99775 AK, USA. [6]Present address: Department of Chemistry and Physics, Mount Royal University, 4825 Mount Royal Gate SW, Calgary T3E 6K6 AB, Canada. ✉e-mail: elspansw@ucalgary.ca

specific passband, at the cost of systematically ignoring other auroral bands (an observational bias). Broadband, panchromatic measurements have also been very successful (e.g. THEMIS all-sky imager) but contain different observational biases, namely that spectral information is integrated and presented as a single luminosity in which relative composition changes cannot be determined. The decades it took the scientific community to recognize STEVE for what it is, and the historical confusion between STEVE and the stable auroral red (SAR) phenomenon[13] expose the drawbacks of the traditional imaging techniques. TREx-RGB, on the other hand, is somewhere in between these two imaging philosophies. The true color profiles reported by TREx-RGB provided the initial motivation for this study and have added data to a previously known, yet dramatically under-sampled, phenomenon.

Like STEVE, the aurora-related continuum emissions examined in this study are not classical auroras but more likely chemiluminescence. However, such chemiluminescence can only be brought into activation or greatly intensified under certain ionospheric/thermospheric conditions induced by previous and/or ongoing magnetospheric energy input and Magnetosphere-Ionosphere-Thermosphere (MIT) coupling (e.g., heating). The investigation of aurora-related continuum emission carried out in this study thus explores a fresh territory of understanding the MIT coupling and its observable consequence in the ionosphere.

In this study, we present observations of continuum emissions that appear to be intimately coupled to auroral dynamics. Our observations are consistent with the unexplained emissions noted by Gattinger and Jones[6] in terms of association with aurora and reported luminosity of continuum emissions (several tens of Rayleighs/nm). Here, we add critical information such as characteristic spatial scale, spectra, and location within auroral dynamics.

Results

Figure 1 provides an overview of 30 such continuum emission events, indicated by the regions encircled by black and white dashed lines, in the TREx-RGB all-sky images. These regions appear as 'grey-toned' or 'white-tinged' structures in the RGB data, corresponding to approximately equal contributions in the red (R), green (G), and blue (B), channels of the RGB sensor. We note that not all regions with nearly equal R, G, and B are associated with continuum emission. The moon, local light sources (e.g., car headlights), and some patchy pulsating auroras produce similar color profiles in the RGB data. All data utilized here are therefore from times in which the moon was below the horizon, and no significant local light sources were noted. The raw data numbers associated with these 'grey-toned' structures are well below the saturation level of the RGB channels. All our identified continuum emission structures are found to be embedded in and/or immediately adjacent to bright auroras, or shortly preceded by bright auroral arcs at essentially the same location. We also note that the continuum emission structures can be associated with a variety of different auroral morphologies.

Figure 2 shows an example of a continuum emission event identified in the co-located spectrograph and RGB camera data. Figure 2a presents a one-hour keogram, which is a north-south slice of the RGB image along its central axis, stacked in time, captured at Rabbit Lake. It illustrates the local auroral activity and structuring surrounding the event timeframe (also see Supplementary Movie 1). The two dashed vertical lines mark the times of the two RGB images shown in Fig. 2b and Fig. 2c. Within the TREx images (Fig. 2b, c) a region of grey-toned luminosity (continuum emission, outlined in black and white) is seen to propagate from west to east bordering a region of bright aurora. As the structure propagates over the spectrograph field of view (N-S oriented line plotted on the RGB images), the observed luminosity spectrum (Fig. 2d) increases at all wavelengths, in a nearly uniform manner. Figure 2d shows the detailed spectrum for the location identified by the dots in Fig. 2b,c. Figure 2b corresponds to the time before the continuum emission structure arrives at the meridian of the spectrograph. This spectrum, shown in orange in Fig. 2d, contains peaks at 557.7 nm and 630.0 nm associated with airglow and weak aurora (not visually apparent on RGB imager without specific contrast adjustment). As the grey-toned structure in RGB propagates towards the meridian imaging spectrograph field of view, the luminosity increases nearly uniformly relative to the earlier time (blue spectra in Fig. 2d). The auroral and airglow signatures are still present in the spectrum, but the background luminosity increases by approximately 20 Rayleigh/nm across all wavelengths as the grey-toned structure approaches zenith. During this event the continuum structure dissipates one minute after the spectrograph observations, with the data only capturing the edge of the structure.

All the event we collected have co-located TREx meridian imaging spectrograph measurements. The spectrograph provides a mechanism to conclusively identify continuum emission within its field of view. To examine the systematic presence of the continuum emission structure, we adopt the following methodology for detection of continuum emission with spectrograph measurements. We utilize the integrated luminosity between 502.0 nm and 507.0 nm, a region of the night-sky spectrum devoid of known airglow and auroral emissions[4]. Figure 3 shows the relative occurrence of 502.0-507.0 nm luminosity, within a single 13 s exposure observed by the TREx meridian imaging spectrograph. TREx-RGB data are also shown for this time (Fig. 3a), with the field-of-view (FoV) of the spectrograph overplotted on the RGB image. Luminosity values in Fig. 3 are color-coded according to the region of the FoV in which they were observed. The grey histogram corresponds to the region poleward of the bright emissions in TREx-RGB. Their spectral intensity (approximately 10-15 Rayleigh/nm) in the 502.0-507.0 nm band is consistent with the reported quiet nightsky intensity composed of ambient continuum, zodiacal light, and starlight[4]. The blue histogram is associated with the region of grey-toned emission in RGB, and the orange histogram corresponds to the region of bright aurora (predominantly green in the TREx-RGB). The region of grey-toned emission in RGB is associated with a statistically different population, containing higher luminosities (> 20 Rayleigh/nm) in the 502.0-507.0 nm passband when compared to regions of aurora or dark sky (as seen in the RGB data). Overall, the luminosity observed in the continuum band ranges between approximately 10–60 Rayleigh/nm in our collected events (see Supplementary Fig. 1). This is well above those reported for ambient continuum emission[4] and is comparable to the unexplained observations of Gattinger and Jones[6] within auroras. However, neither of these previous studies had concurrent 2D auroral images available. The RGB images are therefore capturing the spatial structure of a previously noted, but never spatially resolved, continuum emission associated with auroral dynamics. Here, the spatial structuring (see Fig. 1) is distinctly different from STEVE, in that there appears to be no preferential alignment in longitude or latitude, only a clear association with adjacent auroral activity.

Figure 4 shows the detailed spectra of a grey-toned region within the RGB images corresponding to elevated luminosity in the Sternberg continuum bands. The region of identified continuum emission (white region in the RGB image) is evident based on the near uniform approximately 30 Rayleigh/nm elevation of the spectra (blue line in Fig. 4a) relative to the surrounding regions of bright (orange curve) and no bright (black curve) aurora. Auroral features such as the atomic oxygen 557.7 nm and the N_2^+ first negative group (1NG), appear to be present within the region of grey-toned emission. Since the N_2^+ 1NG requires about 19 eV excitation energy, its presence is usually regarded as a signature of auroral precipitation. In comparison, the STEVE continuum emission is known not to relate to appreciable auroral precipitation[14], evidenced by its much weaker[8,15] 557.7 nm and N_2^+ 1NG intensities than those observed in our continuum structures. Under the assumption that the bright aurora is relatively uniform within the RGB field of view and appears to be present within the region of continuum emission, we attempt to isolate the continuum component of the grey-tone feature by subtracting the bright auroral spectra (orange) from the

https://doi.org/10.1038/s41467-024-55081-5

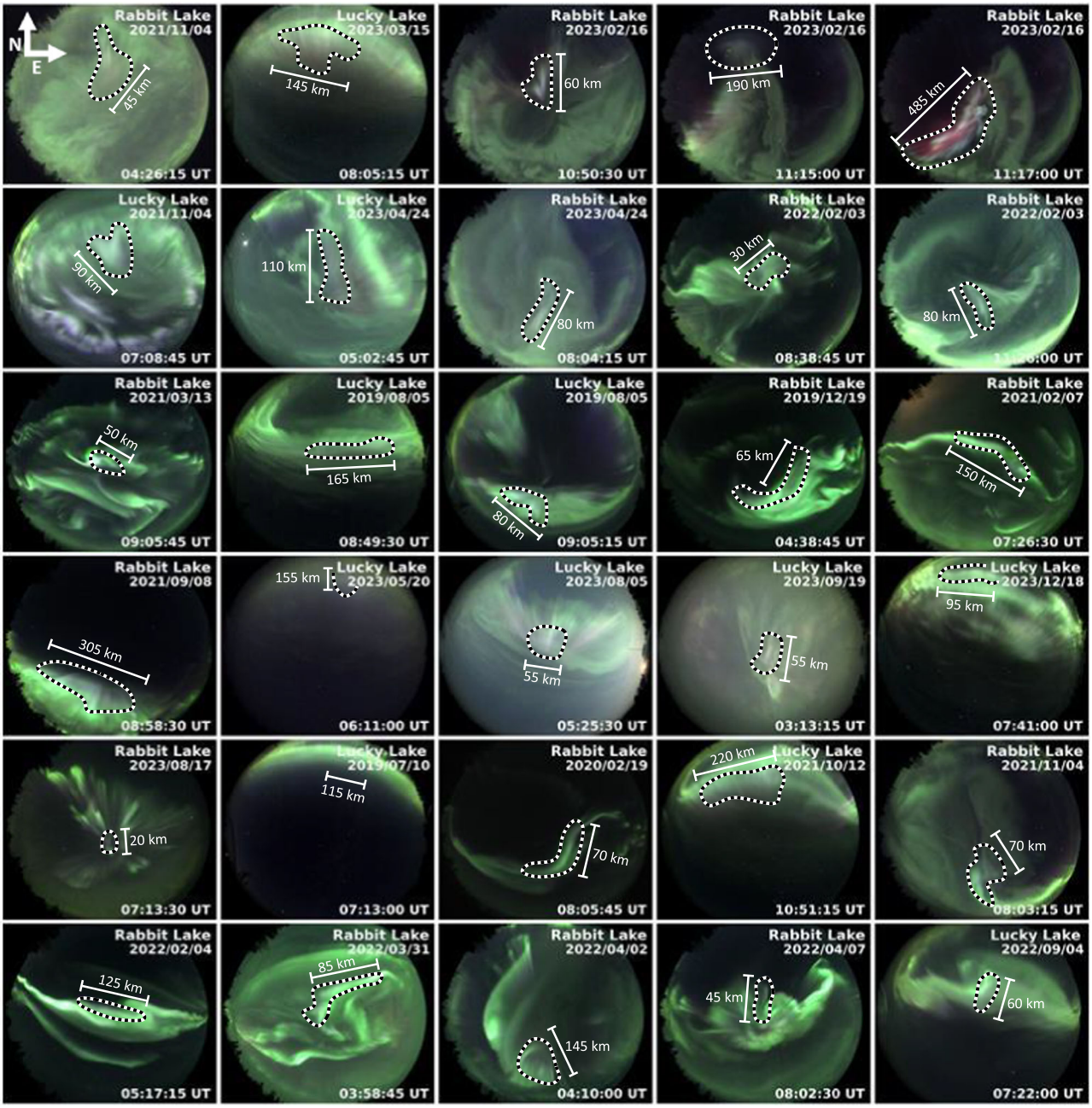

Fig. 1 | Images of structured continuum events and associated aurora. TREx-RGB images showing our identified continuum emission events at Rabbit Lake and Lucky Lake stations. Each event (30 in total) is shown as single image, with the date, time and location shown on the image. Images are plotted in raw format, the color within each image is consistent with a digital photograph and that typically visible with the human eye. In the RGB data, continuum emission appears (outlined by dotted lines where possible) as a white or grey-tone to the observed luminosity, embedded in or alongside the green or red aurora. Orientation of the images is indicated in the top left (N and E are shown). We note the all-sky (fish-eye) lens warps the spatial mapping. In each image, we provide the approximate spatial scale of the continuum structure assuming an altitude of 110 km. Regions of continuum emission are corroborated with the co-located TREx-Spectrograph that provides full spectrum measurements along the (N-S, top-bottom) central meridian of the RGB image.

continuum spectra (blue) to produce a residual spectrum (Fig. 4c). This represents an estimate of the continuum enhancement above and beyond the coincident aurora observed during this time.

Discussion

It can be seen that the difference spectrum consists of a mixture of aurora emission lines/bands and a distinct continuum component. This is a common feature seen in our collected events (see Supplementary Fig. 1). The continuum spectral intensities (a few tens of Rayleigh/nm) in our events are much larger than that found in ambient quiet night sky[4], but are comparable (within a factor of 5) to those reported in conjunction with auroras[5,6] and with STEVE[8,16] We first rule out the possibility of the meteoric metal-induced pseudo-continuum, e.g., FeO or NiO emissions[17,18], since these pseudo-continuum emissions tend to peak around 590–600 nm and diminish rapidly toward blue wavelengths. To date, the most generally accepted explanation of the quiet-time airglow continuum is a chemiluminescent reaction between nitric oxide and oxygen[10,19], i.e., $NO + O^- > NO_2 + h\upsilon$. In Fig. 4c, we overplot the expected spectral profile of such NO_2 continuum emission based on the measurements in Sutoh et al. [20]. by scaling Sutoh et al.'s rate coefficient at 502 nm (i.e., the continuum window) to the observed spectral intensity at the same wavelength. The column

https://doi.org/10.1038/s41467-024-55081-5

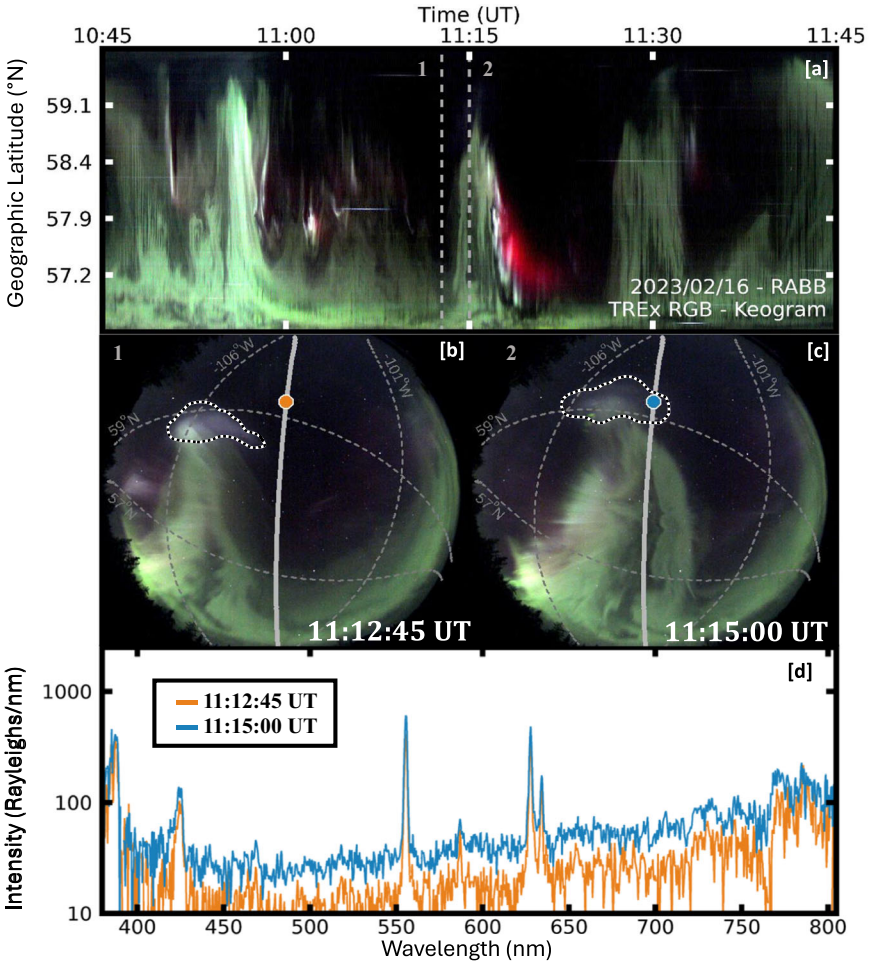

Fig. 2 | Example structured continuum emission event. a One-hour of TREx-RGB data, presented as a keogram, surrounding a structured continuum emission event observed in Rabbit Lake, Saskatchewan on February 16th, 2023. Colors are the same as those recorded in a digital photograph of the night sky with the dynamic aurora indicated by regions of green. The keogram is mapped at 110 km, showing auroral dynamics between 10:45:00 and 11:45:00 Universal Time. Vertical lines (labeled 1 and 2) mark the times of the TREx-RGB images shown in panels b and c respectively. **b** Individual TREx-RGB image from 11:12:45 UT. Contours of constant geographic latitude (degrees North) and longitude (degrees West) at 110 km altitude are shown to provide context for the relative latitudes and separation of the auroral and continuum signatures. Dotted line indicates the region of observed continuum emission. The field of view of the TREx-Spectrograph is indicated by the N-S oriented grey line. The location within the spectrograph FoV identified by the orange circle indicates the location of the spectral measurements shown in panel d. **c** TREx-RGB image in the same format as panel b, but for 11:15:00 UT. The blue circle (same physical location as the orange circle in panel b) indicates the location of the spectral measurements shown in panel d. **d** Detailed spectral measurements at the times of the TREx-RGB images for the location indicated in panels b and c.

[NO][O] density product implied by such scaling is approximately $2\times10^{27}\,cm^{-5}$, compatible with the results in Sharp[5]. Although the rate measurements are only available at several discrete wavelengths, it is theoretically expected that the NO_2 continuum itself does not embed individual N_2 or O emission lines[4,20]. We therefore speculate that the difference spectrum might be explained by a superposition of a NO_2 continuum emission plus multiple auroral/airglow emission lines/bands. These may include a series of the N_2 second positive group (2PG) and N_2+ first negative group (1NG) emissions in the blue wavelength range, the N_2 first positive group in the near-infrared range, and enhanced Oxygen lines 557.7/630.0 nm. The presence of strong auroral precipitation in the continuum is conducive to electronic/vibrational excitation of N_2 and NO production[21,22]. In this regard, we note that some of the higher-vibration-level N_2 2PG and N_2^+ 1NG emission bands (see labels in Fig. 4c), which are weak in ordinary auroras[23], become strongly enhanced in the continuum. We, however, admit that, due to the incomplete knowledge of the nature of the continuum and its characteristic spectrum, it is uncertain from the current study whether such enhanced N_2 emission bands are an intrinsic part of the continuum itself or caused by other related yet separate processes. This will be examined in future studies.

To summarize, with a unique combination of RGB imager and spectrograph observations enabled by the TREx mission, we survey and investigate the 'grey-toned' structures characterized by continuum emissions in the auroral region, with details and breadth unparalleled in the preexisting literature. These grey-toned structures range in size from 10 s to 100 s of km (Fig. 1). They are embedded in and/or preceded by active auroras (high contrast structures varying on timescale of minutes or less), and their spectra contain distinguishable auroral emission components, indicating that auroral energy deposition is a key factor in their formation. However, they are not pure auroras but contain a distinct continuum emission component. We propose that such continuum emission structures stem from a co-play and coupling among auroral excitation, disturbed ionospheric/thermospheric conditions (e.g., heating), and a chemiluminescent continuum. A NO_2 continuum is considered as one potential candidate for the observed continuum. The dynamic variation, meso-scale morphology, and contextualization with auroral structures, distinguish our observed continuum emission structures from those previously-studied ambient NO_2 continuum or STEVE. The findings reported in this letter, and the large database of continuum emissions achieved from this study, enable us and the community to venture into a fresh research territory of mesoscale

https://doi.org/10.1038/s41467-024-55081-5

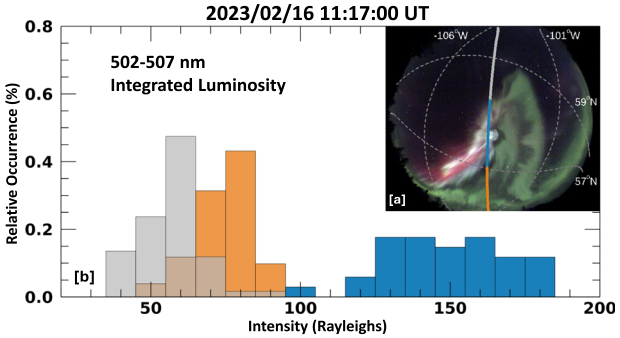

Fig. 3 | Relative occurrence of continuum emission luminosities. a Single TREx-RGB image from Rabbit Lake taken on Feb 16th, 2023, at 11:17:00 UT. The field of view of the N-S aligned TREx-Spectrograph is shown as a line. The spectrograph FoV is color-coded according to the type of luminosity being observed. Blue is the region of identified continuum emission, orange is a dynamic auroral region, and grey is a region of dark sky (as observed by the TREx-RGB). Colors within the TREx-RGB image are the same as those recorded in a digital photograph, with the aurora being predominantly green or red. Contours of constant geographic latitude (degrees North) and longitude (degrees West) at 110 km altitude are shown to provide context for the relative latitudes and separation of the auroral and continuum signatures. **b** Relative occurrence of integrated luminosities in the 502-507 nm band of the TREx-Spectrograph. The colors of the histogram populations correspond to their respective locations in the image shown in panel a.

coupling among auroral precipitation, the ionosphere, and the thermosphere, leading to chemiluminescent continuum. Case studies of the continuum emission with ancillary observations (e.g., in-situ measurements of plasma/neutrals), as well as modeling studies of the coupling among auroral precipitation, ionospheric/thermospheric heating, and the excited neutral constituents relevant to responsible for the continuum emission, would advance our understanding of the MIT processes leading to the continuum emission.

Methods

TREx-RGB employs a highly sensitive color CMOS (Complementary Metal-Oxide-Semiconductor) sensor, capable of 3 Hz imaging at near 100% duty cycle. The nominal imaging mode for TREx-RGB is to average nine 3 Hz frames together to provide a 3 s cadence data product, in true color. The operational stability (across temperature, time, within the FoV, etc.) and repeatability of color response (across sensors) of the commercial CMOS cameras is the enabling factor used here to distinguish relative changes in emission color and quantify its associated spatial structure within the aurora. We limit this study to data from the Rabbit Lake and Lucky Lake TREx-RGB systems. Both cameras have co-located TREx meridian imaging spectrographs. The TREx-spectrographs simultaneously image a meridional slice of the night sky covering 180 degrees (horizon to horizon) aligned in the N-S direction. Each spectrograph takes 15 s images (with 13 s integration), producing a complete spectrum from approximately 400 to 800 nm (0.4 nm resolution), for each look

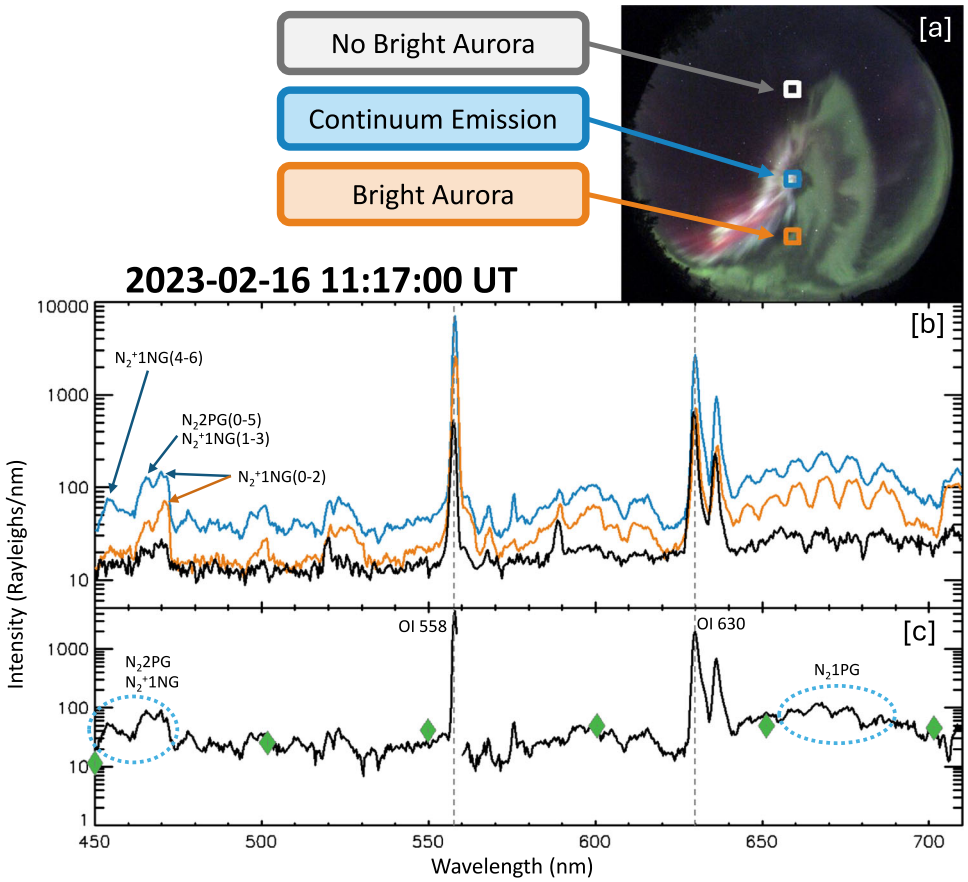

Fig. 4 | Estimate of continuum emission spectrum. a Single TREx RGB image from Rabbit Lake taken on 2023-02-16, at 11:17:00 UT (same image as Fig. 3). The locations of the three regions analyzed are shown in white (no bright aurora, predominantly dark sky in the RGB data), blue (region of grey-toned, continuum emission) and orange (region of bright aurora, predominantly green in the RGB data). **b** The optical spectra corresponding to each of the highlighted regions in panel a. **c** A residual spectrum of the continuum enhancement is estimated by subtracting the bright auroral spectra (orange) from the continuum spectra (blue) to produce an estimated spectrum associated with the grey-toned enhancement above and beyond the auroral spectra. The relative luminosity of the continuum spectra presented by Sutoh et al.[19]. (scaled to match the observed spectra intensity) is overplotted as green diamonds. Spectral regions of interest are labeled in both the original (panel b) and residual (panel c) spectra.

direction (1-degree resolution along the N-S scan, with an approximate width of 3 degrees)[8]. Each TREx spectrograph is fully calibrated[8] to provide quantitative luminosity measurements of the spectral composition. To characterize the continuum emission, we utilize the wavelength band between 502.0 nm and 507.0 nm, a region of the night-sky spectrum devoid of known airglow and auroral emissions. Our chosen passband is within previously identified wavelength regimes used for studies of continuum emission (namely, 501.4–518.7 nm, see Table 2 of ref. 4).

Data availability

The list of events used in this study is included in the Supplementary Material. The processed TREx Spectrograph data used for each event is available at https://data.phys.ucalgary.ca/sort_by_project/other/publication_datasets/2024SpanswickContinuum/. RGB data is used in it's raw format. Full data access to the TREx-Spectrograph [https://doi.org/10.11575/2wnp-yc80] and RGB [https://doi.org/10.11575/4p8e-1k65] datasets are available via the University of Calgary Open Science Platform (https://data.phys.ucalgary.ca). Direct data archive access is available via http, ftp, or an API (please see documentation provided on http://data.phys.ucalgary.ca). Data is organized by site (location), and time of observation (as provided in the Supplementary Material). The datasets generated during and/or analysed during the current study are available from the corresponding author upon request. Source data are provided with this paper.

References

1. Noxon, J. F. Day airglow. *Space Sci. Rev.* **8**, 92–134 (1968).
2. Young, R. A. Chemiluminescent reactions in the airglow. *J. Chem. Can.* **47**, 1927–1937 (1969).
3. Barbier, D., Dufay, J. & Williams, D. Recherches sur l'émission de la raie verte de la lumière du Ciel nocturne. *Ann. Astrophys.* **14**, 399–437 (1951).
4. Sternberg, J. R. & Ingham, M. F. Observations of the airglow continuum. *Mon. Not. R. astr. Soc.* **159**, 1–20 (1972).
5. Sharp, W. E. NO2 continuum in aurora. *J. Geophys. Res.* **83**, 4373–4376 (1978).
6. Gattinger, R. L. & Jones, A. V. Quantitative spectroscopy of the aurora. II. the spectrum of medium intensity aurora between 4500 and 8900 Å. *Can. J. Phys.* **53**, 2343–2356 (1974).
7. MacDonald, E. A. et al. New science in plain sight: Citizen scientists lead to the discovery of optical structure in the upper atmosphere. *Sci. Adv.* **4**. https://doi.org/10.1126/sciadv.aaq0030 (2018).
8. Gillies, D. M. et al. First observations from the TREx spectrograph: The optical spectrum of STEVE and the picket fence phenomena. *Geophys. Res. Lett.* **46**. https://doi.org/10.1029/2019GL083272 (2019).
9. Liang, J. et al. Optical spectra and emission altitudes of double-layer STEVE: A case study. *Geophys. Res. Lett.* **46**, 13630–13639 (2019).
10. Harding, B. J., Mende, S. B., Triplett, C. C. & Wu, Y. J. A mechanism for the STEVE continuum emission. *Geophys. Res. Lett.* **47**. https://doi.org/10.1029/2020GL087102 (2020).
11. Nishimura, Y., Dyer, A., Kangas, L., Donovan, E. & Angelopoulos, V. Unsolved problems in Strong Thermal Emission Velocity Enhancement (STEVE) and the picket fence. *Front. Astron. Space Sci.* **10**. https://doi.org/10.3389/fspas.2023.1087974 (2023).
12. Spanswick, E. & Donovan, E. Transition Region Explorer - RGB Dataset. University of Calgary. https://doi.org/10.11575/4P8E-1K65.
13. Hunnekuhl, M. & MacDonald, E. Early ground-based work by auroral pioneer Carl Størmer on the high-altitude detached subauroral arcs now known as "STEVE. *Space Weather* **18**, e2019SW002384 (2020).
14. Gallardo-Lacourt, B., Liang, J., Nishimura, Y. & Donovan, F. On the origin of STEVE: Particle precipitation or ionospheric skyglow? *Geophys. Res. Lett.* **45**, 7968–7973 (2018).
15. Mende, S. B., Harding, B. J. & Turner, C. Subauroral green STEVE arcs: Evidence for low-energy excitation. *Geophys. Res. Lett.* **46**, 14256–14262 (2019).
16. Gillies, D. M., Liang, J., Gallardo-Lacourt, B. & Donovan, E. New insight into the transition from a SAR arc to STEVE. *Geophys. Res. Lett.* **50**. https://doi.org/10.1029/2022GL101205 (2023).
17. Evans, W. F. J. et al. Discovery of the FeO orange bands in the terrestrial night airglow spectrum obtained with OSIRIS on the Odin spacecraft. *Geophys. Res. Lett.* **37**. https://doi.org/10.1029/2010GL045310 (2010).
18. Evans, W. F. J., Gattinger, R. L., Broadfoot, A. L. & Llewellyn, E. J. The observation of the chemiluminescent NiO* emissions in the laboratory and in the night airglow. *ACP* **11**, 9595–9603 (2011).
19. Hedin, J., Rapp, M., Khaplanov, M., Stegman, J. & Witt, G. Observations of NO in the upper mesosphere and lower thermosphere during ECOMA 2010. *ANGEO* **30**, 1611–1621 (2012).
20. Sutoh, M., Morioka, Y. & Nakamura, M. Absolute rate constant for the chemiluminescent reaction of atomic oxygen with nitric oxide. *J. Chem. Phys.* **72**, 20–24 (1980).
21. Campbell, L., Cartwright, D. C. & Brunger, M. J. Role of excited N2 in the production of nitric oxide. *J. Geophys. Res.* **112**, A08303 (2007).
22. Campbell, L., Cartwright, D. C., Brunger, M. J. & Teubner, P. J. O. Role of electronic excited N2 in vibrational excitation of the N2 ground state at high latitudes. *J. Geophys. Res.* **111**, A09317 (2006).
23. Blasko, J., Orszagh, J., Stachova, B. & Matejcik, S. Spectral electron energy map of electron impact induced emission of nitrogen. *Eur. Phys. J. D* **77**. https://doi.org/10.1140/epjd/s10053-023-00602-y (2023).

Acknowledgements

The Transition Region Explorer is a joint Canada Foundation for Innovation and Canadian Space Agency project developed by the University of Calgary. The TREx RGB and Spectrograph instruments are operated and maintained by Space Environment Canada with the support of the Canadian Space Agency (CSA) [23SUGOSEC].

Author contributions

E.S.: study lead, oversight, study design, data analysis, and manuscript writing. J.L.: detailed spectral analysis and modeling, manuscript writing. JH: spectrograph and RGB analysis, contributed to manuscript preparation. D.C.: contributed to analysis and database of events presented in study, contributed to manuscript. E.D. & B.G.L.: contributed to study direction, contributed to manuscript. C.K. & J.R.: performed preliminary RGB analysis and contributed to manuscript. Y.N.: contributed to discussion of phenomena and contributed to manuscript. D.H. and M.G.: provided base code for spectrograph calibration and contributed to manuscript.

Competing interests

The authors declare no competing interests.

Additional information

Supplementary information The online version contains supplementary material available at https://doi.org/10.1038/s41467-024-55081-5.

Correspondence and requests for materials should be addressed to E. Spanswick.

Peer review information *Nature Communications* thanks the anonymous reviewers for their contribution to the peer review of this work. A peer review file is available.